ELSEVIER

Contents lists available at ScienceDirect

# Journal of Water Process Engineering

journal homepage: www.elsevier.com/locate/jwpe



# A water treatment method utilizing a continuous flow material recovery system to facilitate removal of contaminant ions

Teagan J. Leitzke <sup>a,\*</sup>, Jerome P. Downey <sup>a</sup>, Richard M. LaDouceur <sup>b</sup>, Grant C. Wallace <sup>a</sup>, Katie J. Schumacher <sup>a,c</sup>, Morgan R. Ashbaugh <sup>d</sup>, David L. Hutchins <sup>a</sup>

- <sup>a</sup> Metallurgical and Materials Engineering, Montana Technological University, 1300 W. Park St. Butte, MT 59701, USA
- <sup>b</sup> Mechanical Engineering, Montana Technological University, 1300 W. Park St. Butte, MT 59701, USA
- <sup>c</sup> Materials Science Ph.D. Program, Montana Technological University, 1300 W. Park St. Butte, MT 59701, USA
- <sup>d</sup> Materials Science and Engineering M.S. Program, Montana Technological University, 1300 W. Park St. Butte, MT 59701, USA

#### ARTICLE INFO

#### Keywords: Contaminant removal Magnetic separation Magnetite Adsorption Water treatment

## ABSTRACT

A continuous flow material recovery (CFMR) system was investigated for use in tandem with a magnetite (Fe<sub>3</sub>O<sub>4</sub>) adsorbent for the removal of contaminant ions from waters. The CFMR was assessed by examining the effects of flow rate, Cu(II) concentration, and Fe<sub>3</sub>O<sub>4</sub> dose. Experiments indicated that low flow rates, under 3 Lpm, were ideal for minimizing release of Fe<sub>3</sub>O<sub>4</sub> and maximizing saturation time of the Fe<sub>3</sub>O<sub>4</sub> capture system. Over 98 % Fe<sub>3</sub>O<sub>4</sub> recovery was observed near ideal conditions. Further experimentation revealed Fe<sub>3</sub>O<sub>4</sub> capture efficiencies between 38 and 93 %, Cu(II) removal between 80 and 99 %, and loading up to 20 mg Cu(II)/g Fe<sub>3</sub>O<sub>4</sub>. Additionally, magnetite adsorption was evaluated by treating water samples from the Clark Fork River, located in southwestern Montana. Many contaminants tested were removed to below water quality criteria or instrument detection limits. This study poses a potential solution for water pollution, with the ability to be modified for applications such as environmental remediation and wastewater treatment, and demonstrates an efficient water treatment process for real-world applications. Ultimately, the study aims to establish CFMR operating conditions that minimize Fe<sub>3</sub>O<sub>4</sub> loss to the environment and assess Fe<sub>3</sub>O<sub>4</sub> adsorption capabilities on real water samples.

#### 1. Introduction

Natural waters and anthropogenic wastewaters can contain trace levels of toxic materials, such as metals and nutrients. Metals exposure can occur due to natural phenomenon, such as erosion or volcanic eruptions, or anthropogenic activities, including industrial operations, electroplating, and mining [1–6]. Nutrient contamination can be caused by anthropogenic sources, including food product processing and agricultural or storm water runoff, and geogenic sources [7–11]. Humans, aquatic life, plant life, and the environment can be detrimentally affected by exposure to toxic materials, including cancer, organ damage, and eutrophication [3,6,8,10–12]. Contaminated waters pose crucial threats to human health, aquatic and plant life, and the environment, leading to the need for an efficient and effective method for contaminant removal.

Researchers are utilizing conventional technologies and developing new technologies to address and facilitate contaminant removal. These technologies include coagulation, sedimentation, high gradient magnetic separation, membrane bioreactor technologies,

electro-adsorption, and reverse osmosis [13–17]. Research involving new contaminant removal technologies have limited knowledge of large-scale use and continuous operation, mostly performing on the laboratory-scale [13,18,19]. The continuous flow material recovery (CFMR) system discussed in this work provides a simple and efficient method for wastewater treatment, compared to other technologies, utilizing magnetite (Fe $_3$ O $_4$ ) as an adsorbent and fills in some of the knowledge gap for large-scale, continuous operation for contaminant removal processes. In addition, the compact system can be modified for differing scales of operation, with the option of using it on-site so transport of contaminated waters to a treatment facility is not needed. Continuous operation of the system is also advantageous, especially for processing large volumes of water at industrial scales.

Further, in real-world applications, treated water will be released back into the environment, so ensuring environmental concerns are not associated with the system is essential. One major concern is loss of  $Fe_3O_4$  into the environment, especially

E-mail address: tleitzke@mtech.edu (T.J. Leitzke).

<sup>\*</sup> Corresponding author.

contaminant-loaded Fe $_3$ O $_4$ . Loaded Fe $_3$ O $_4$  are of concern as they may become unstable and leach adsorbed contaminants back into the environment. Magnetic properties of Fe $_3$ O $_4$  allow for simple and efficient collection by the CFMR system, reducing chemicals required for removal and production of secondary pollutants, and additional measures utilizing permanent magnets can be installed to ensure minimal Fe $_3$ O $_4$  loss [5,20–23]. Overall, the CFMR system represents a user-friendly, efficient, and effective method for low-level contaminant removal and recovery from wastewaters.

This work used a novel CFMR system in a series of experiments designed to evaluate its ability to effectively capture contaminant-loaded  $Fe_3O_4$  particles from a feed stream. Magnetite adsorption on real water samples was also explored by treating water samples obtained from the Clark Fork River (CFR), which is of importance due several factors, including high metals contamination from hard rock mining in the area, it forms the headwaters for the Colombia River system, and it is the largest river in Montana by volume [24]. Experiments included flow-through and continuous CFMR operation, and single- and

multi-stage adsorption. Models for CFMR operation were generated and validated using a central composite design with response surface methodology in Design-Expert® 12, a logistic regression analysis software. The CFMR system was the focus of experimentation to demonstrate an efficient and effective water treatment process for real-world applications, specifically in contaminated tributaries that feed into larger rivers and industrial applications, and to expand upon previous work done by the authors [20,21,25,26].

#### 2. Materials and equipment

Experiments in this work used commercially available Fe $_3O_4$  purchased from U.S. Research Nanomaterials (Fe $_3O_4$ , 98 + %, 20–30 nm). A MIRA3 TESCAN scanning electron microscope (SEM) was used to obtain images of the sample, where a variety of morphologies are apparent, observed in Fig. 1, contrasting vendor size specifications and potentially

caused by agglomeration during drying of the Fe<sub>3</sub>O<sub>4</sub>.

Surrogate solutions (solutions prepared in the laboratory with known concentrations) were prepared with copper(II) sulfate pentahydrate (CuSO $_4$ •5H $_2$ O) purchased from Sigma Aldrich and samples were analyzed with an iCAP 6500 Series inductively coupled plasma-optical emission spectrometer (ICP-OES). Water samples were collected from the Clark Fork River (CFR) at Arrow Stone Park in Deer Lodge, Montana and analyzed by the Montana Bureau of Mines and Geology using an iCAP Q inductively coupled plasma-mass spectrometer (ICP-MS) for trace metal analyses. All samples were preserved for analysis using nitric acid (HNO $_3$ ) for trace metals analysis from J.T. Baker.

The CFMR used is the 5th iteration of the system design. The 5th generation design fixes problems in previous designs, including adsorbent settling and size. A magnetic collection module containing an electromagnet was chosen for the design to separate contaminant-loaded  $Fe_3O_4$  from the feed due to ease of separation compared to use of permanent magnets.

A Sartorius Corporation Practum 224-1S Balance (max 220 g) or Denver Instrument APX-1502 Analytical Balance (max 1500 g) were used to weigh  $Fe_3O_4$  and  $CuSO_4 \bullet 5H_2O$ .

#### 3. Methods

## 3.1. CFMR experiments

## 3.1.1. Flow-through experiments

Flow-through experiments were conducted to determine optimal operating conditions for the CFMR. Key operating parameters include breakthrough time (defined as time when particles were observed in the effluent stream), flow rate, and  $\rm Fe_3O_4$  dose. Breakthrough was chosen as a parameter for experiments because any accidental release of contaminant-loaded  $\rm Fe_3O_4$  could cause environmental problems due to the potential for leaching; knowledge of the breakthrough time is essential to prevent the electromagnet (EM) from becoming saturated

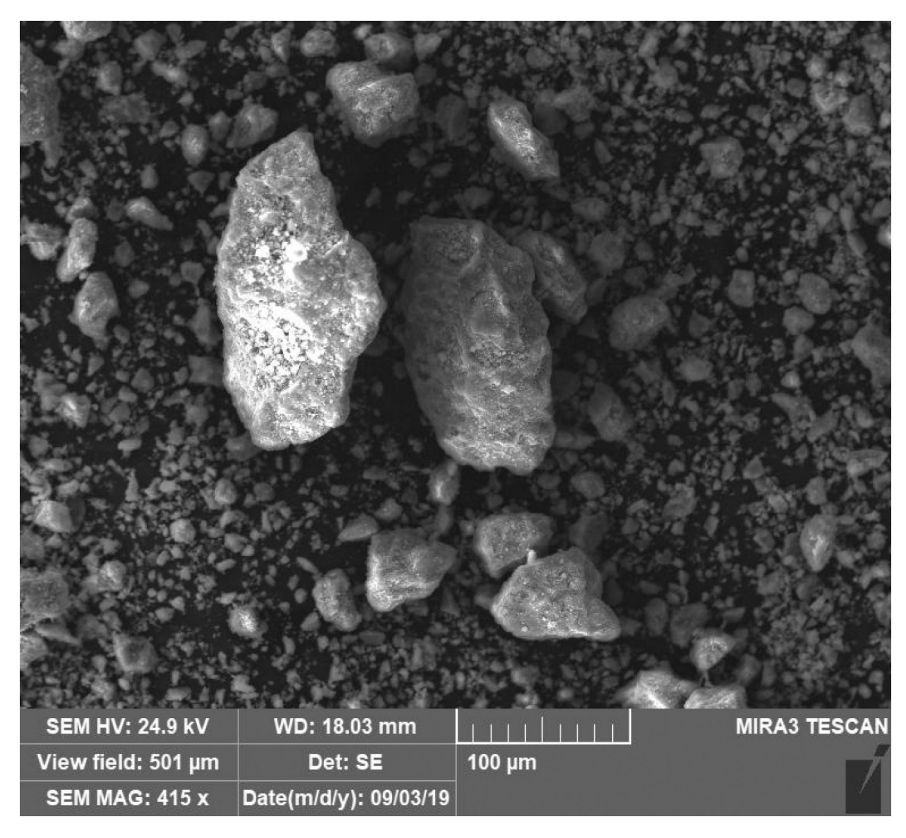


Fig. 1. SEM image of Fe<sub>3</sub>O<sub>4</sub> particles from U.S. Research Nanomaterials at 415× magnification.

and to establish electromagnet cycles when multiple magnetic collection modules are used. From prior experimentation, it was determined that the EM must produce at least 1 kG of electromotive force to achieve sufficient magnetite capture, therefore EM strength was not examined as a parameter for these experiments [25].

Design-Expert® 12 was used to develop a statistical design of experiments using a central composite design with response surface methodology to identify optimal conditions for CFMR operation and minimize  $Fe_3O_4$  loss (defined as amount of  $Fe_3O_4$  entering the effluent stream). A series of 13 experiments, supplemented by two confirmation experiments, were conducted to determine the effects of flow rate and  $Fe_3O_4$  dose on CFMR operation in

flow-through mode, and the setup is presented in Fig. 2. Flow and dose were varied from 1.0 to 3.4 Lpm and 6 to 20 g Fe $_3$ O $_4$ /L, respectively. Understanding the effects of and interactions between these parameters on Fe $_3$ O $_4$  capture in the CFMR will identify ideal operating conditions and enable improved design and scale-up of the CFMR system.

Flow-through experiments were performed under central composite design conditions for a duration of 5 min, and the procedure is as follows. Slurries were prepared by mixing Fe<sub>3</sub>O<sub>4</sub> and deionized water (DI), agitating until completely dispersed. The EM was then turned on and the slurry was poured into the CFMR through the funnel. Simultaneously, the valve at the end of the system, valve 2 in Fig. 2, was opened and flow was adjusted using valve 1 in Fig. 2. As each experiment progressed, the time at which Fe<sub>3</sub>O<sub>4</sub> was seen in the end bucket, indicating Fe<sub>3</sub>O<sub>4</sub> breakthrough, was recorded. After 5 min, indicating the end of each experiment, the flow was stopped, EM de-energized, and breakthrough Fe<sub>3</sub>O<sub>4</sub> was collected from the end bucket. Breakthrough Fe<sub>3</sub>O<sub>4</sub> was magnetically separated from the water, dried in air, and weighed to assess EM operation under varying magnetite concentrations and flow rates. The CFMR was flushed with DI between experiments until water from the valves ran clean. All experiments were conducted at room temperature and ambient pressure. A more detailed description and diagram of the CFMR process can be found in Supplementary Material (SM) Text S1 and Fig. S1.

### 3.1.2. Continuous operation experiments

Continuous operation experiments examined the effects of  $Fe_3O_4$  dose, flow rate, and Cu(II) concentration and assessed the system's ability to perform for an extended period of time. Dose, flow rate, and Cu(II) concentration were varied from 140 to 200 g  $Fe_3O_4$  /L, 1 to 4 Lpm, and 100 to 500 mg Cu/L, respectively. Copper(II) was chosen as the contaminant for these studies as it is the most prominent contaminant in the authors' location. Duplicates of 3 experiments were conducted and the setup is presented in Fig. 3. Continuous operation of the CFMR relies on utilizing a parallel or series configuration of multiple replicate magnetic collection modules, so demonstration of only a single collection module is necessary. In practice, the CFMR system would be comprised of multiple electromagnets in a parallel or series configuration. Understanding the effects of operation parameters in continuous mode will enable improved design of the CFMR system.

The procedure for continuous experiments is as follows. Solutions were prepared by dissolving CuSO<sub>4</sub>•5H<sub>2</sub>O in DI and pouring the solution into the feed tank. Magnetite was added to the tank, and the slurry mixed at 800  $\pm$  10 rpm for 5 min prior to beginning the experiment to start Cu(II) adsorption onto Fe<sub>3</sub>O<sub>4</sub>. The pump was then turned on, flow adjusted, and EM energized. At 20 min intervals, flow was stopped to flush the EM, which was deenergized to release captured Fe<sub>3</sub>O<sub>4</sub>, with DI. Twenty-minute intervals were chosen due to the time required to flush the magnet (5-7 min) and lack of system automation. Flow was then restarted and EM reenergized. The Cu(II) solution was recycled through the CFMR over the 10 h period, and loss of solution or addition of DI from EM flushes were assumed to be negligible. Copper(II) solutions were cycled to accommodate limitations of the current CFMR setup, including size and use of only one magnetic collection module, and to minimize the volume of solution required for the experiments. Contaminant concentration and pH were recorded at specific sampling times over the course of 10 h. Magnetite captured by the EM over the 10 h was collected on a permanent magnet, air dried, and weighed to determine removal efficiency. For all experiments, all glassware and sample storage vials were triple rinsed with 5 % HNO<sub>3</sub>, then triple rinsed with 18 M $\Omega$  DI to minimize contamination. Between experiments, the CFMR tank was scrubbed, and the entire system was flushed with DI. All

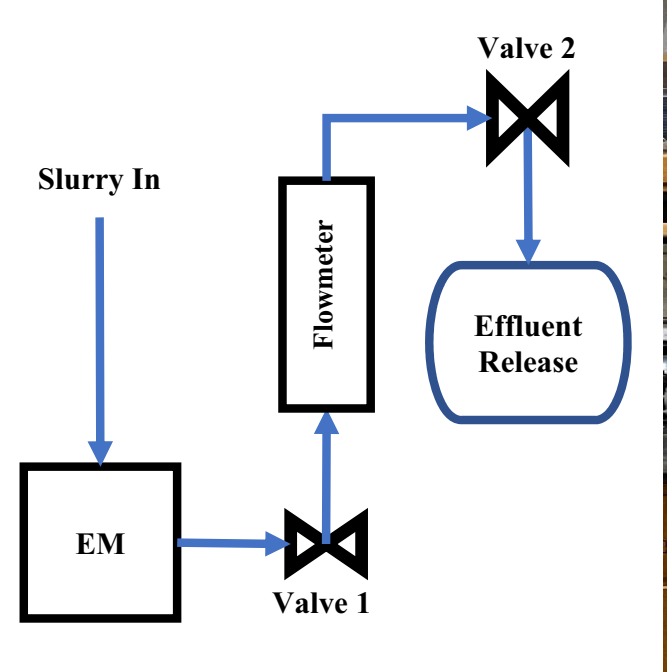




Fig. 2. Continuous flow material recovery experimental setup for flow-through operation. Schematic at left and physical setup at right.



Fig. 3. Continuous flow material recovery experimental setup for continuous operation. The setup includes a mechanical mixer, feed tank, pump apparatus, electromagnet, power supply, tubing to recycle the water, and tubing to flush the electromagnet with deionized water.

experiments were conducted at room temperature, intrinsic pH, and ambient pressure. All water samples were analyzed by ICP-OES.

From these data, removal efficiency for Cu(II) removal and  $Fe_3O_4$  capture can be calculated and is given by Eq. 1

$$\%Removal = \frac{(C_0 - C_e)}{C_0} *100 \tag{1}$$

where  $C_0$  and  $C_e$  are the initial and final concentrations, in mg/L for Cu (II) removal and g for Fe<sub>3</sub>O<sub>4</sub> capture [27]. Removal efficiency expresses the percentage removed from the system by comparing initial and final concentrations. Contaminant loading, q, can also be calculated, using Eq. 2

$$q = \frac{(C_0 - C_e)^* V}{m} \tag{2}$$

where  $C_0$  and  $C_e$  are the initial and final concentrations (mg/L), V is the volume (L), and m is the mass of adsorbent (g). Contaminant loading expresses the amount of adsorbate taken up by the adsorbent per unit mass (or volume) of the adsorbent.

## 3.2. Single- and multi-stage adsorption experiments

Single- and multi-stage adsorption experiments were performed on water samples from the CFR to assess  $Fe_3O_4$  adsorption capabilities in real water samples. Prior experimentation by the authors had established  $>\!95$  % removal of Cu(II), Pb(II), or  $PO_4^{3^-}$  in surrogate solutions, therefore water samples with many mixed elements was ideal for assessing viability of  $Fe_3O_4$  for real-world applications [26]. For all experiments, all glassware and sample storage vials were triple rinsed with 5 % HNO\_3, then triple rinsed with 18 M $\Omega$  DI to minimize potential contamination. Additionally, all experiments were conducted at intrinsic pH, room temperature, and ambient pressure. All samples were analyzed by an iCAP Q ICP-MS.

The procedure for single-stage removal is as follows.  $500\ mL$  of CFR water was measured into a  $1\ L$  beaker, and initial solution pH was

recorded. The beaker was then placed under mechanical agitation at 400 rpm. Magnetite was weighed and added to the solution at approximately 20 g/L for all experiments. After 1 h of mixing, final pH was recorded and a sample taken. Samples were immediately filtered and preserved with  $HNO_3$ .

The procedure for multi-stage removal is the same as the procedure described in the previous paragraph with the addition of three subsequent stages, which are as follows. After

1~h of mixing, pH was measured and a 40 mL sample was taken, filtered, and preserved with HNO3. A permanent magnet was then used to separate  $Fe_3O_4$  from the depleted solution which was decanted into another 1~L beaker. The beaker was placed back under mechanical agitation at 400 rpm, and a fresh mass of  $Fe_3O_4$  was added to the solution and mixed for another hour. The process was repeated for all stages with 1~h of mixing between stages.

# 4. Results and discussion

# 4.1. CFMR experiments

#### 4.1.1. Flow-through experiments

A statistical design of experiments based on a central composite design was generated to optimize the flow of feed into the CFMR system in relation to  $Fe_3O_4$  breakthrough and  $Fe_3O_4$  loss. The design consisted of two numerical factors, flow and  $Fe_3O_4$  dose, and two responses,  $Fe_3O_4$  breakthrough and  $Fe_3O_4$  loss to the treated stream. The results of the 13 experiments were input into the Design-Expert® 12 experimental design for analysis by the software. An automatic model selection using Akaike's information criterion estimates the quality of each model compared to the other models and determines which terms to keep in the model. A reduced quadratic model with a base 10 log transform was chosen as the best model for the breakthrough data, while a reduced quadratic model with an inverse square root transform was chosen for the  $Fe_3O_4$  model. Once the models have been generated, an analysis of variance (ANOVA) performs statistical tests, where p-values <0.05 of

the model and <0.1 of the variables suggest significance. Table 1 and Table 2 display the ANOVA results and fit statistics for both models. ANOVA of the breakthrough model, at top in Table 1, indicates that the model and all factors are significant, while the Fe<sub>3</sub>O<sub>4</sub> loss model, at top in Table 2, indicates that the model, flow, and quadratic of Fe<sub>3</sub>O<sub>4</sub> dose are significant, while Fe<sub>3</sub>O<sub>4</sub> dose is not significant, but due to the quadratic being significant, Fe<sub>3</sub>O<sub>4</sub> dose must be included in the model. Fit statistics, which aid in determining model quality, display positive results for both models. In both cases, agreement between  $R^2$ , adjusted  $R^2$ , and predicted  $R^2$  suggests that the models fit the data and can interpolate points. Additionally, adequate precision, which assess signal-to-noise ratio, indicates strong signals for model optimization. Overall, ANOVA and fit statistics indicate the generated models are a good fit for the data.

Further, diagnostics reveal supplementary information about trends, outliers, and influences on the model (SM Text S2 and Fig. S2). One additional plot is the interaction plot, which aids in establishing behavior of the responses and numerical factors, presented in

Fig. 4. At left in Fig. 4, the breakthrough model reveals that flow rate does not have a significant impact on breakthrough time at high doses Fe<sub>3</sub>O<sub>4</sub>, while slower flows result in longer breakthrough times at low Fe<sub>3</sub>O<sub>4</sub> doses. These results make sense because high Fe<sub>3</sub>O<sub>4</sub> doses would saturate the EM more quickly, and high flows would result in faster breakthrough at low Fe<sub>3</sub>O<sub>4</sub> doses. The Fe<sub>3</sub>O<sub>4</sub> loss model, at right in Fig. 4, reveals that Fe<sub>3</sub>O<sub>4</sub> dose does not have a significant effect on Fe<sub>3</sub>O<sub>4</sub> loss, as the design points and 95 % confidence interval bands lie near each other. These results indicate that the EM is not reaching saturation at the Fe<sub>3</sub>O<sub>4</sub> doses used and higher doses would be needed to significantly affect Fe<sub>3</sub>O<sub>4</sub> loss. The generated models establish optimal conditions of 1 Lpm to maximize Fe<sub>3</sub>O<sub>4</sub> breakthrough time and near 2.8 Lpm to minimize  $Fe_3O_4$  loss. The small-scale conditions under which these experiments were performed result in flows that are ideal for treating small streams and tributaries, but by expanding the ranges of the parameters, operation of the CFMR system would be better informed for large-scale and industrial applications.

Additionally, two confirmation points were chosen from a list generated by

Design-Expert® 12 to evaluate the predictive capabilities of the model and statistically validate it. Confirmation point experiments were conducted using the method described in 3.2.1. The first experiment was

**Table 1** ANOVA and fit statistics for breakthrough.

ANOVA for reduced quadratic model with base 10 log transform						
Source	Sum of Squares	df	Mean Square	F-value	P-value	
Model	1.58	4	0.3949	73.50	< 0.0001	Significant
A –	1.18	1	1.18	219.37	< 0.0001	
Flow						
B -	0.1692	1	0.1692	31.50	0.0005	
$Fe_3O_4$						
AB	0.1614	1	0.1614	30.04	0.0006	
$B^2$	0.0703	1	0.0703	13.09	0.0068	
Residual	0.0430	8	0.0054			
Lack of	0.0116	4	0.0029	0.3715	0.8197	Not
Fit						significant
Pure	0.0313	4	0.0078			
Error						
Cor	1.62	12				
Total						
Fit Statisti	cs					
Std. Dev.	0.0733			$R^2$	0.9735	
Mean	1.53			Adjusted R <sup>2</sup>	0.9603	
C.V. %	4.80			Predicted R <sup>2</sup>	0.9455	
				Adeq Precision	30.1988	

**Table 2**ANOVA and fit statistics for Fe<sub>3</sub>O<sub>4</sub> loss.

Source	Sum of Squares	df	Mean Square	F-value	P-value	
Model	0.9335	3	0.3112	62.03	< 0.0001	Significant
A – Flow	0.8742	1	0.8742	174.26	< 0.0001	
B – Fe <sub>3</sub> O <sub>4</sub>	0.0008	1	0.0008	0.1575	0.7007	
$B^2$	0.0585	1	0.0585	11.66	0.0077	
Residual Lack of Fit	0.0452 0.0221	9 5	0.0050 0.0044	0.7641	0.6199	Not significant
Pure Error	0.0231	4	0.0058			0
Cor Total	0.9786	12				
Fit Statistic	rs					
Std. Dev.	0.0708			$\mathbb{R}^2$	0.9539	
Mean	0.7058			Adjusted R <sup>2</sup>	0.9385	
C.V. %	10.03			Predicted R <sup>2</sup>	0.9115	
				Adeq Precision	23.8189	

conducted using 6 g Fe $_3$ O $_4$ /L and 1.9 Lpm, and the second experiment used 20 g Fe $_3$ O $_4$ /L and 3.0 Lpm. Duplicate experiments were performed for each point and the confidence interval data is presented in Table 3, where it can be observed that the data mean values are all within the 95 % prediction intervals (PI). Due to equipment limitations and current experimental setup, high variability was apparent while conducting the experiments, but model refinement may be achieved with system automation and improved experimental setup. Therefore, it was concluded that the range of PIs were acceptable and confirmation points indicate acceptable models.

## 4.1.2. Continuous operation experiments

Continuous operation experiments were conducted to evaluate the CFMR system in terms of  $Fe_3O_4$  capture and Cu(II) removal and assess performance over an extended period of time. Experiments were conducted using 10 L of Cu(II) solution, agitation speed of

 $800\pm10$  rpm,  $Fe_3O_4$  doses of 140 g/L for CF-1 and CF-2, 200 g/L for CF-3 and CF-4, and

170 g/L for CF-5 and CF-6, and initial copper concentrations of 100 mg/L for CF-1 and CF-2, 500 mg/L for CF-3 and CF-4, and 200 mg/L for CF-5 and CF-6. Experiments were performed at intrinsic pH, which ranged from 5.32 to 4.17, depending on  $CuSO_4 \bullet 5H_2O$  concentration.

Table 4 displays  $Fe_3O_4$  capture from the EM at the end of each 10 h continuous flow (CF) experiment. The high- and mid-range  $Fe_3O_4$  dose experiments at low and high flows, respectively, resulted in recoveries of 83 % on average, whereas the low-range dose and

mid-range flow experiments resulted in low recovery of 38 %. Ideally,  $Fe_3O_4$  recovery would approach 90+%, and potential causes for loss or low recoveries are  $Fe_3O_4$  loss through the EM (indicating a stronger EM may be necessary), caught in the system, or stuck within the EM coils. Another cause may be due to recycling the water, which increased in temperature to approximately  $57\,^{\circ}\text{C}$  by the end of the experiments, potentially oxidizing  $Fe_3O_4$  surfaces to hematite  $(Fe_2O_3)$  or converting a percentage to  $Fe_2O_3$ , which is non-magnetic [28,29]. In real-world applications, water would not be recycled and adding additional collection modules should alleviate heating problems. Ultimately, improvements to the CF setup based on these findings should be considered to minimize  $Fe_3O_4$  loss.

Further, Cu(II) removal was monitored over the course of the 10 h experiments. Results for duplicate experiments were averaged and data is presented in Fig. 5, with error bars for percent removal representing a

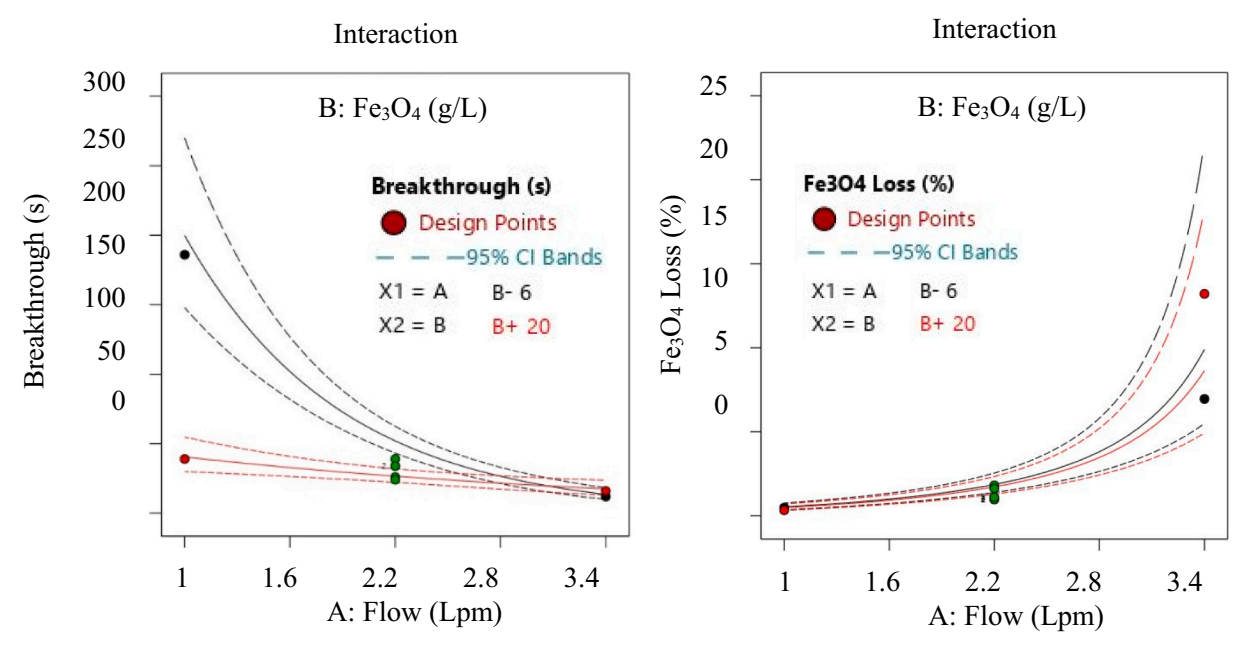


Fig. 4. Interaction plots for the magnetite breakthrough (left) and loss (right) models.

**Table 3**CFMR Design of Experiments Confirmation Points.

	-			
Response	Confirmation Point	95 % PI Low	Data Mean	95 % PI High
Breakthrough	1	51.29	52.66	100.48
ьгеакшгоцуп	2	0.79	1.54	2.22
Fo O Loss	1	13.74	21.45	28.63
Fe <sub>3</sub> O <sub>4</sub> Loss	2	2.26	3.88	9.31

**Table 4** Fe<sub>3</sub>O<sub>4</sub> capture from CF experiments.

Trial	Flow Rate	Fe <sub>3</sub> O <sub>4</sub> Dose	Captured	Fe <sub>3</sub> O <sub>4</sub> Recovered
	(Lpm)	(g)	Fe <sub>3</sub> O <sub>4</sub> (g)	(%)
CF – 1 and CF – 2	$2.2\pm0.2$	280	106.03	37.87
CF – 3	$1.0 \pm 0.2$	200	160.88	80.44
CF – 4		200	168.71	84.36
CF – 5	$4.0\pm0.2$	170	158.38	93.16
CF – 6		170	129.17	75.98

standard percent error based on slight drift of the continuous calibration verification samples from the ICP-OES.

Copper(II) removal data, displayed in Fig. 5, reveals high removal efficiencies for all experiments. As expected, low  $C_0$  resulted in the highest removal efficiency of 99 %, while the highest  $C_0$  achieved a removal efficiency of 80 %. Some discrepancies are observed near the beginning of the experiments and are assumed to be caused by nonhomogeneous mixing, as some Cu(II) solution flowed into the pump system before starting, resulting in slightly fluctuating Cu(II) concentrations in the first several data points. Further, initial adsorption occurs rapidly for the lowest Cu(II) concentration, while it takes approximately 3 h for higher concentration experiments to achieve over 60 % Cu(II) removal, and loading reached a maximum of 20 mg Cu(II)/g  $Fe_3O_4$ . These results indicate that increased  $Fe_3O_4$  doses are required to improve removal efficiencies, especially at high contaminant concentrations, and reduce Cu(II) concentrations below water quality criteria (WQC) of 2.85  $\mu$ g/L at 25 mg/L hardness [30,31].

Further, pH data is displayed as an insert to Fig. 5 and reveals an overall decrease in pH over the course of the experiments. Final

concentrations were 4.77, 3.94, and 4.11 for experiments CF-1/2, CF-3/4, and CF-5/6, respectively. Additional information on pH for the CF experiments can be found in SM Text S3, Fig. S3, and Table S1.

## 4.2. Magnetite adsorption experiments

Single-stage (SS) and multi-stage (MS)  $Fe_3O_4$  adsorption experiments were conducted to evaluate  $Fe_3O_4$  performance on real water samples containing a variety of contaminant ions. Trials labelled with a U represent untreated samples, representing the initial sample concentration, and trials labelled 1–4 represent the experimental stage number, where the final stage represents the final concentration. Triplicate experiments were performed on CFR water samples using 20 g  $Fe_3O_4/L$ , with averages and standard deviations presented in Table 5. Water quality criteria, displayed in Table 5, were obtained from DEQ-7 and WHO guidelines and dashes indicate no value given [30,31].

Table 5 presents excellent removal for selected contaminants. Initial concentrations for Zn, As, Sr, Sb, and Ba were already below WQC, but were reduced by  $Fe_3O_4$  adsorption by approximately 85 %, 98 %, 78 %, 60 %, and 97 %, respectively. Data for additional elements can be found in SM Text S4 and S5 and Tables S2 and S3. Ultimately,  $Fe_3O_4$  performance on CFR samples displays highly promising results for application as the adsorbent media for use in the CFMR system.

# 5. Conclusions

A CFMR system was evaluated in flow-through and continuous operation to establish ideal operating conditions and assess performance for an extended time. Statistical models for flow-through experiments indicated that flows around 1.0 Lpm are ideal to maximize Fe<sub>3</sub>O<sub>4</sub> breakthrough time and under 2.8 Lpm to minimize Fe<sub>3</sub>O<sub>4</sub> loss. Continuous experiments revealed Fe<sub>3</sub>O<sub>4</sub> capture efficiencies between 37 % and 93 % and Cu(II) removal between 80 % and 99 %. Expanding parameter ranges for CFMR experiments to explore ideal large-scale operating conditions and incorporating automation into CFMR system to further refine statistical models should be considered for future studies. Water samples from the CFR were treated with Fe<sub>3</sub>O<sub>4</sub> to assess adsorption capabilities in natural waters and display promising results, as many of the contaminants tested were removed to below water quality criteria or below instrument detection limits. Overall, results from this study reveal

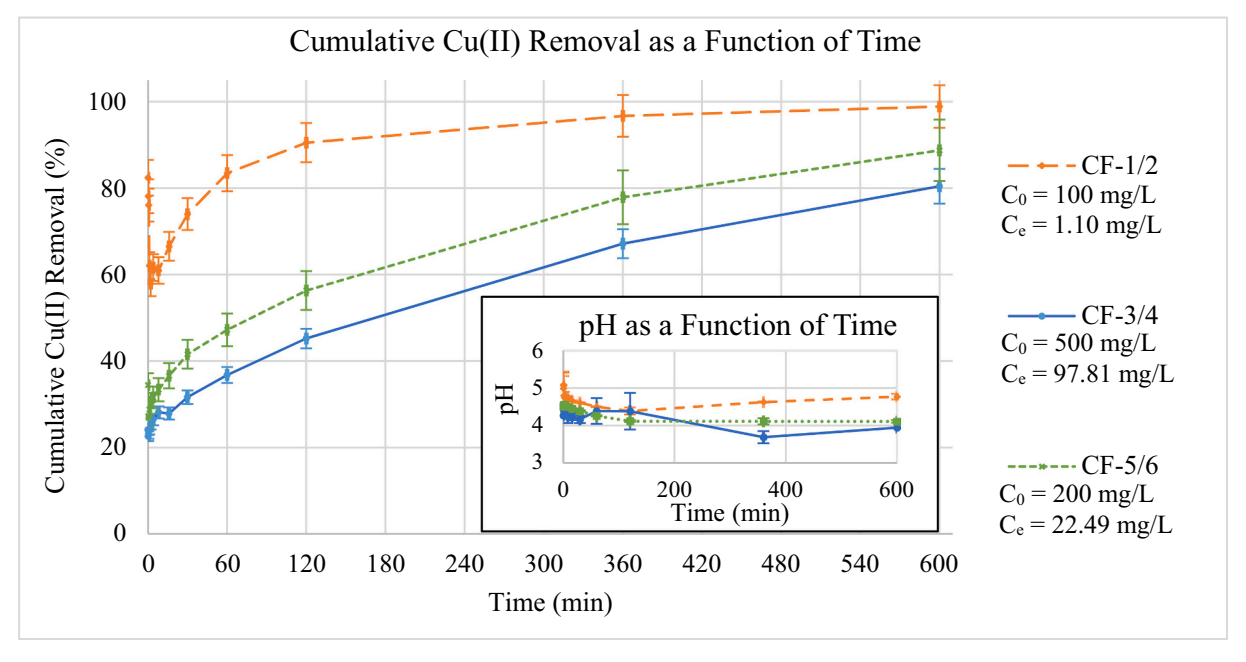


Fig. 5. Averaged cumulative copper removal efficiencies for duplicate 10 h continuous flow experiments. Insert: Average pH for duplicated 10 h continuous flow experiments (additional information available in SM Text S3, Fig. S3, and Table S1). The lines connecting the data are for visual purposes only.

Table 5
CFR adsorption ICP-MS data.

Element	Zn (μg/ L)	As (μg/ L)	Sr (μg/L)	Mo (μg/ L)	Sb (µg/ L)	Ba (μg/ L)
Trial						
MS – U	8.71 $\pm$	9.49 $\pm$	263.61 $\pm$	24.65 $\pm$	0.49 $\pm$	33.76 $\pm$
	0.29	0.12	2.01	0.12	0.02	0.26
MS-1	$\begin{array}{c} 1.37 \; \pm \\ 0.09 \end{array}$	< 0.2	$58.19 \pm 2.44$	< 0.5	< 0.2	< 1
MS-2	$\begin{array}{c} 1.55 \pm \\ 0.15 \end{array}$	< 0.2	$12.62 \pm \\1.43$	< 0.5	< 0.2	< 1
MS - 3	$\begin{array}{c} 1.70 \; \pm \\ 0.23 \end{array}$	< 0.2	$3.66 \pm 0.59$	< 0.5	< 0.2	< 1
MS-4	$\begin{array}{c} 1.17 \; \pm \\ 0.04 \end{array}$	< 0.2	$\begin{array}{c} 1.84 \pm \\ 0.37 \end{array}$	< 0.5	< 0.2	< 1
00 11	$9.09 \pm$	9.73 $\pm$	279.91 $\pm$	25.74 $\pm$	$0.5 \pm$	34.10 $\pm$
SS – U	0.45	0.09	10.65	0.76	0.01	0.05
SS - 1	$\begin{array}{c} \textbf{1.43} \pm \\ \textbf{0.05} \end{array}$	< 0.2	$60.53 \pm \\1.33$	< 0.5	< 0.2	< 1
WQC	37	150	20	-	0.5	3

that the CFMR process may be a promising and simple solution to water pollution. Additionally, the process can be modified for a variety of water treatment applications, including environmental remediation and prevention of contaminant release from industrial or municipal wastewaters.

# Role of the funding source

This material is based upon work supported in part by the National Science Foundation EPSCoR Cooperative Agreement *OIA-1757351*. NSF EPSCoR were not involved in the conceptualization of the study design; in the collection, analysis, and interpretation of data; in the writing of the report; nor in the decision to submit the article for publication.

# Declaration of competing interest

The authors declare that they have no known competing financial interests or personal relationships that could have appeared to influence the work reported in this paper.

## Data availability

Data will be made available on request.

#### Acknowledgements

The authors would like to thank Daisy Margrave for obtaining SEM images and Jackie Timmer and Ashley Huft of the Montana Bureau of Mines and Geology for analyzing CFR water samples.

This material is based upon work supported in part by the National Science Foundation EPSCoR Cooperative Agreement OIA-1757351. Any opinions, findings, and conclusions or recommendations expressed in this material are those of the author(s) and do not necessarily reflect the views of the National Science Foundation.

## Appendix A. Supplementary data

CFMR Process Description (Text S1); CFMR Process Diagram (Fig. S1); Design-Expert® 12 Diagnostics Plot Descriptions (Text S2); Design-Expert® 12 Diagnostics Plots (Fig. S2); pH Description (Text S3); pH Graph (Fig. S3); pH Table (Table S1); CFR ICP-MS Data Analysis (Text S4); CFR ICP-MS Data (Table S2); Water Quality Criteria (Text S5); and Water Quality Criteria Sources and Values (Table S3). Supplementary data to this article can be found online at doi:https://doi.org/10.1016/j.jwpe.2023.104546.

# References

- E. Vunain, A.K. Mishra, B.B. Mamba, Dendrimers, mesoporous silicas and chitosanbased nanosorbents for the removal of heavy-metal ions: a review, Int. J. Biol. Macromol. 86 (2016) 570–586, https://doi.org/10.1016/j.ijbiomac.2016.02.005.
- [2] P.B. Tchounwou, C.G. Yedjou, A.K. Patlolla, D.J. Sutton, in: A. Luch (Ed.), Heavy Metal Toxicity and the Environment, Springer, Basel, 2012, pp. 133–164, https://doi.org/10.1007/978-3-7643-8340-4-6.
- [3] E. Ghasemi, A. Heydari, M. Sillanpää, Superparamagnetic Fe3O4@EDTA nanoparticles as an efficient adsorbent for simultaneous removal of Ag(I), Hg(II), Mn(II), Zn(II), Pb(II) and Cd(II) from water and soil environmental samples, Microchem. J. 131 (2017) 51–56, https://doi.org/10.1016/j.microc.2016.11.011.
- [4] J.M. Besser, K.J. Leib, Toxicity of metals in water and sediment to aquatic biota, in: S.E. Church, P. von Guerard, S.E. Finger (Eds.), Integrated Investigations of Environmental Effects of Historical Mining in the Animas River Watershed, San Juan County, Colorado, U.S. Geological Survey, 2007, pp. 837–849. Accessed: Sep.

- 22, 2022. [Online]. Available: https://pubs.usgs.gov/pp/1651/downloads/Vol2 combinedChapters/vol2 chapE19.pdf.
- [5] Z. Cheng, A.L.K. Tan, Y. Tao, D. Shan, K.E. Ting, X.J. Yin, Synthesis and characterization of iron oxide nanoparticles and applications in the removal of heavy metals from industrial wastewater, International Journal of Photoenergy 2012 (2012) 1–5, https://doi.org/10.1155/2012/608298.
- [6] R. DeMars, Health hazards from mining in Butte, Montana, in: Teach the Earth, 2016. https://serc.carleton.edu/68792 (accessed Apr. 21, 2022).
- [7] M. Jaishankar, T. Tseten, N. Anbalagan, B. B. Mathew, and K. N. Beeregowda, "Toxicity, mechanism and health effects of some heavy metals," Interdiscip. Toxicol., vol. 7, no. 2, pp. 60–72, Jun. 2014, doi:https://doi.org/10.2478/intox-2 014-0009
- [8] S. Ebrahimi and D. J. Roberts, "Sustainable nitrate-contaminated water treatment using multi cycle ion-exchange/bioregeneration of nitrate selective resin," J. Hazard. Mater., vol. 262, pp. 539–544, Nov. 2013, doi:https://doi.org/10.1016/j. jhazmat.2013.09.025.
- [9] D.-W. Cho, H. Song, B. Kim, F. W. Schwartz, and B.-H. Jeon, "Reduction of nitrate in groundwater by Fe(0)/magnetite nanoparticles entrapped in ca-alginate beads," Water Air Soil Pollut., vol. 226, no. 7, p. 206, Jul. 2015, doi:https://doi.org/10.100 7/s11220.015-2467.6
- [10] T. Nur, M. A. H. Johir, P. Loganathan, T. Nguyen, S. Vigneswaran, and J. Kandasamy, "Phosphate removal from water using an iron oxide impregnated strong base anion exchange resin," J. Ind. Eng. Chem., vol. 20, no. 4, pp. 1301–1307, Jul. 2014, doi:https://doi.org/10.1016/j.jiec.2013.07.009.
- [11] U.S. Environmental Protection Agency, Nutrient Indicators Dataset, U.S. Environmental Protection Agency, 2020. https://www.epa.gov/nutrient-policy-data/nutrient-indicators-dataset (accessed Oct. 21, 2022).
- [12] Y.-S. Kim et al., "Simultaneous removal of phosphate and nitrate in wastewater using high-capacity anion-exchange resin," Water Air Soil Pollut., vol. 223, no. 9, pp. 5959–5966, Nov. 2012, doi:https://doi.org/10.1007/s11270-012-1331-1.
- [13] C. D. Powell et al., "Magnetic nanoparticle recovery device (MagNERD) enables application of iron oxide nanoparticles for water treatment," J. Nanopart. Res., vol. 22, no. 2, p. 48, Feb. 2020, doi:https://doi.org/10.1007/s11051-020-4770-4.
- [14] B. Arnsten, Designing an integrated wastewater-treatment system, Chemical Engineering 127 (9) (2020) 39–44. Accessed: Oct. 11, 2022. [Online]. Available: https://www.chemengonline.com/designing-integrated-wastewater-treatment-system/.
- [15] S. Zhang et al., "Research progress, problems and prospects of mine water treatment technology and resource utilization in China," Crit. Rev. Environ. Sci. Technol., vol. 50, no. 4, pp. 331–383, Feb. 2020, doi:https://doi.org/10.1080/10 643389 2019 1620708
- [16] M. Mao, T. Yan, G. Chen, J. Zhang, L. Shi, D. Zhang, Selective capacitive removal of Pb 2+ from wastewater over redox-active electrodes, Environ. Sci. Technol. 55 (1) (Jan. 2021) 730–737. https://doi.org/10.1021/acs.est.0c06562.
- [17] M. Mao, T. Yan, J. Shen, J. Zhang, D. Zhang, Selective capacitive removal of heavy metal ions from wastewater over Lewis Base sites of S-doped Fe-N-C cathodes via an electro-adsorption process, Environ. Sci. Technol. 55 (11) (Jun. 2021) 7665–7673, https://doi.org/10.1021/acs.est.1c01483.

- [18] F. Younas, et al., Current and emerging adsorbent technologies for wastewater treatment: trends, limitations, and environmental implications, Water (Basel) 13 (2) (Jan. 2021) 215, https://doi.org/10.3390/w13020215.
- [19] S. Shibatani, et al., Study on magnetic separation device for scale removal from feed-water in thermal power plant, IEEE Trans. Appl. Supercond. 26 (4) (Jun. 2016) 1–4, https://doi.org/10.1109/TASC.2016.2523433.
- [20] T. Leitzke, J. P. Downey, D. Hutchins, and B. St. Clair, Continuous Flow Process for Removal and Recovery of Water Contaminants with Magnetic Nanocomposites. 2019. doi:https://doi.org/10.1007/978-3-030-35790-0\_13.
- [21] D.L. Hutchins, J.P. Downey, Effective separation of magnetite nanoparticles within an industrial-scale pipeline reactor, Sep. Sci. Technol. 55 (15) (Oct. 2020) 2822–2829, https://doi.org/10.1080/01496395.2019.1646762.
- [22] S. Rajput, C.U. Pittman, D. Mohan, Magnetic magnetite (Fe3O4) nanoparticle synthesis and applications for lead (Pb2+) and chromium (Cr6+) removal from water, J. Colloid Interface Sci. 468 (Apr. 2016) 334–346, https://doi.org/10.1016/ LJCIS 2015 12 2008
- [23] Y. Kalpakli, Removal of Cu (II) from aqueous solutions using magnetite: a kinetic, equilibrium study, Adv. Environ. Res. 4 (2) (Jun. 2015) 119–133, https://doi.org/ 10.12989/aer.2015.4.2.119.
- [24] Clark Fork Coalition, "About our watershed," 2022. https://clarkfork.org/ (accessed Sep. 14, 2022).
- [25] D. Hutchins, Continuous Flow Process for Recovery of Metal Contaminants from Industrial Wastewaters with Magnetic Nanocomposites, Ph.D. Thesis, Montana Technological University, 2018. Accessed: Oct. 19, 2022. [Online]. Available: https://digitalcommons.mtech.edu/grad\_rsch/183.
- [26] T. Leitzke, J. Downey, R. LaDouceur, D. Margrave, G. Wallace, D. Hutchins, Water treatment method for removal of select heavy metals and nutrient ions through adsorption by magnetite, ACS ES&T Water 2 (9) (2022) 1584–1592, https://doi. org/10.1021/acsestwater.2c00242.
- [27] J.C. Crittenden, R. Trussell, D. Hand, K. Howe, G. Tchobanoglous, Water Treatment: Principles and Design, 3rd ed., John Wiley & Sons, Inc., Hoboken, NJ, 2012.
- [28] Z. Li, C. Chanéac, G. Berger, S. Delaunay, A. Graff, G. Lefèvre, Mechanism and kinetics of magnetite oxidation under hydrothermal conditions, RSC Adv. 9 (58) (2019) 33633–33642, https://doi.org/10.1039/C9RA03234G.
- [29] S.P. Schwaminger, D. Bauer, P. Fraga-García, F.E. Wagner, S. Berensmeier, Oxidation of magnetite nanoparticles: impact on surface and crystal properties, CrystEngComm 19 (2) (2017) 246–255, https://doi.org/10.1039/C6CE02421A.
- [30] Montana Department of Environmental Quality, Planning Prevention and Assistance Division, Water Quality Planning Bureau, and Water Quality Standards Section, DEQ-7 Montana Numeric Water Quality Standards, Montana Dept. of Environmental Quality, 2012. https://www.epa.gov/sites/production/files/ 2014-12/documents/mt-deq7.pdf (accessed Oct. 18, 2022).
- [31] World Health Organization, Guidelines for Drinking-Water Quality: Fourth Edition Incorporating the First Addendum, World Health Organization, 2017. https://apps. who.int/iris/bitstream/handle/10665/254637/9789241549950eng.pdf;jsessioni d=81A6462C6B69DEC89868A049F48C305A?sequence=1 (accessed Oct. 24, 2022)